IEEE *Access*

Multidisciplinary : Rapid Review : Open Access Journal

Power Reduction Estimation of 5G Active Antenna Systems for Human Exposure Assessment in Realistic Scenarios

MARCO D. MIGLIORE[1],(SENIOR MEMBER, IEEE), AND FULVIO SCHETTINO[1],(Member, IEEE)

[1]DIEI (Department of Electrical and Information Engineering 'Maurizio Scarano'), ICEmB (Centro nazionale di ricerca Interuniversitario sulla Interazioni fra Campi Elettromagnetici e Biosistemi) and ELEDIA@UniCAS - University of Cassino and Southern Lazio, via G. Di Biasio 43, 03043 Cassino, Italy (e-mail mdmiglio@unicas.it, schettino@unicas.it)

Corresponding author: Marco Donald Migliore (e-mail: mdmiglio@unicas.it).

ABSTRACT Maximum power extrapolation techniques from measured data are usually employed to assess the compliance with standards of average fields radiated by base stations. However, such techniques provide an upper bound, which is not reached in real scenarios. This is particularly true in 5G Communications, where Active Antenna Systems allow a decrease of the average power density according to the adopted scheduling strategy. This paper is focused on the power reduction estimation in realistic scenarios. In particular a deterministic model of a communication system is used to obtain simple formulas only requiring the knowledge of the served area angular extension and of the Envelope Radiation Pattern of the antenna.

The model, developed for beam steering and grid of beams antennas, is also extended to analyze the case of Multi User massive Multiple Input Multiple Output (MU-mMIMO) antennas with single layer per user, showing that under proper hypothesis on the beams of the antenna it is possible to estimate the reduction parameter without the explicit knowledge of the number of layers of MU-mMIMO systems.

In spite of the simplicity of the approach, comparison with stochastic models and results reported in recent literature show that the formulas obtained using the model proposed in this paper allow to obtain a useful approximation of the power reduction factor, making the formulas suitable for a preliminary fast estimation of the Electromagnetic Field in 5G cells for human exposure assessment.

INDEX TERMS Antenna arrays, Antenna radiation pattern, 5G Systems, Beam steering, Grid of Beams, Exposure Limits, Massive MIMO

I. INTRODUCTION

5G is designed to meet the rapidly growing demand for high bit rate, low latency and high reliability communications. Compliance with the 5G specifications required unprecedented efficiency in the use of the resources made available by the wireless communication channel. Indeed, in addition to a flexible use of time resources, obtained by a number of new concepts such as flexible numerologies and Bandwidth Parts [1], 5G is characterized by an aggressive use of space resources based on beamforming and MIMO antennas [2], [3]. Although some of these solutions have been also pro-

posed in 4G, they represent a key technology in 5G [1], [4].

Past studies on advanced antennas were mainly focused on the maximization of data throughput of the communication system, whereas investigation on the electromagnetic level in the environment in 5G cells was object of relatively little research.

With the implementation of 5G systems a new phase has started and nowadays the estimation of the Electromagnetic Field (EMF) of 5G signals for human exposure assessment is attracting the attention of a growing number of researchers [5]–[11].

The approach currently investigated to handle this problem is based on two steps [12]. The first step is the Maximum Power Extrapolation (MPE) procedure, and allows to estimate the maximum power that can be received starting from the measured data. The value obtained from the MPE procedure is an unrealistic upperbound, since it supposes that all the resources of the communication system are given to only one user. This quantity is then multiplied by a proper correction factor taking into account the stochastic nature of the problem in order to obtain a realistic value [5]–[8]. This paper is focused on this second step.

The main contribution of this work is represented by some simple analytical formulas approximating the reduction factor for the assessment of human exposure determined by the use of Active Antenna Systems (AAS) in 5G base stations. Unlike other methods, requiring a detailed knowledge of the antenna patterns, the proposed formulas only require the knowledge of the Envelope Radiation Pattern, also called envelope of beams.The Envelope Radiation Pattern, as defined in Sect. 2.9 of [13], is a "non-physical radiation pattern obtained by taking, for each direction in azimuth and elevation, the maximum of the absolute, not peak normalized, radiation pattern among the radiation patterns that the AAS can generate", and is an information on antennas that vendors are expected to provide.In this paper the reduction factor is evaluated in terms of power density. It is understood that, if required, the reduction in terms of EMF can be straightforwardly evaluated as the square root of the reduction factor in terms of power density.

It is useful to note that this paper considers only the effect of antennas. Indeed, 5G introduces some extra characteristics besides antennas that significantly impact the EMF level, and in particular a large variation of the BS radiated power, roughly proportional to the amount of data to be transmitted in the cell [1]. This last feature is predominant in the EMF reduction in case of few users and in general when the percentage of used Resource Blocks in the 5G frame is low. The role of antennas instead becomes predominant in case of full use of the frame resources. Accordingly, the aim of this paper is the estimation of the antenna effect in case of a *large number of users*. However, for sake of completeness, the case of small number of users will also be discussed, being useful for a complete understanding of the impact of antennas in 5G EMF level.

The approach proposed in this paper compares the EMF level on a Reference User (RU) connected to the Base Station (BS) 5G antenna with the EMF level radiated by an isotropic BS antenna using a simplified deterministic communication system model. The formulas are valid under some assumptions about the BS antenna beams that is useful to discuss in some details.

Loosely speaking, a 5G antenna is not characterized by a single pattern, but by a set of different patterns. 5G standard includes specific procedures to handle the selection of the most suitable pattern for user connection based on two steps [1], [14]. The first step uses the SS-PBCH signals, that are transmitted by a set of moderately directive beams called 'broadcast beams', able to cover the entire region served by the BS. The second step is based on the CSI-RS (Channel State Information Reference Signal), that is used by the User Equipment (UE) to measure the channel. As response to a received CSI-RS, the UE sends a CSI report containing a number of information including the index of the best antenna precoding matrix among a codebook of possible antenna precoding matrices available at the BS. These precoding matrices are associated to high directivity patterns, called 'traffic beams'. Consequently, the BS has a set of possible patterns (i.e. a 'grid of beams' as the set of beams is called in 5G literature) among which a specific pattern is selected.

Antennas used in currently deployed 5G systems are basically planar arrays using precoding matrices generally based on DFT processing [15]. Accordingly, in this paper we consider equispaced planar arrays radiating a 'grid of beams', as well as beam steering antennas (whose main lobe exactly points toward the RU position). The analysis is also extended to the case of MU-mMIMO, whose use in deployed 5G systems is imminent, approximating the field radiated by the BS antenna as a superposition of the fields obtained using beam-forming technique for each user.

In addition to numerical simulations carried out specifically to verify the deterministic model, the results of the simple formulas obtained in this paper are also compared with the ones reported in the current literature, based on highly accurate numerical simulations and extensive experimental measurements [5]–[8]. The numerical and experimental methods followed in the above referenced papers allow to obtain the power reduction factor at 95th percentile (F_{pr}, [12]) that is used to evaluate a realistic value of the EMF level starting from the value estimated by maximum power extrapolation methods [16]–[20], as indicated by the norms.

It is understood that the formulas obtained in this paper are based on a deterministic model that is only a "rough approximation" of the sophisticated stochastic models used in the above referenced paper. However, in spite of the simplicity of the approach, the comparison will show that the formulas obtained using the simple deterministic model proposed in this paper are able to give a rough but still useful approximation of the reduction factor for all the antenna systems considered in this paper, making the formulas suitable for a preliminary fast evaluation of the effect of the EMF level in 5G cells.

II. EMF POWER DENSITY REDUCTION USING BEAM STEERING ANTENNAS

In a Beam Steering antenna the main lobe points exactly toward the user to be served.

In this Section we will analyze the impact of the use of Beam Steering antennas on the field level using a simplified 2D deterministic free space propagation model. This case is at the basis of all the other antenna systems discussed in the paper. For the sake of completeness, beside the case of a
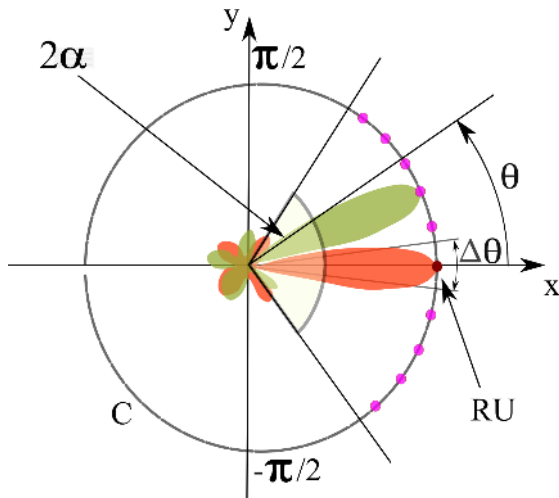
FIGURE 1. The 2D model consists of a large number P of users (drawn as colored circles on the circumference C), each covering an angular region $\Delta\theta$ in the $(-\alpha, \alpha)$ angular range; N users out of P are served in the unit time, including the RU user (RU, drawn as red circle); $M = (P-1)/(N-1)$ units of times are required to serve all the P users; the figure shows the pattern pointing along the RU (red pattern) and the pattern pointing toward a different user (green pattern); all the possible radiated patterns are supposed symmetric with respect to the main lobe and equal apart from an angular rotation.

large number of users, that is the main goal of this paper, in this Section the case of a small number of users will also be analyzed.

We consider a BS working at wavelength λ placed at the center of a circumference C whose radius is large compared to the wavelength (Fig. 1). P users are placed on an arch $(-\alpha, \alpha)$ of the circumference C at angular positions θ_i, $i = 1, ..., P$. Since all the users are on C, the distance from the BS is equal for any user, and will be dropped in the following for simplicity of notation. Furthermore, we suppose that the BS does not suffer from any ohmic losses so that Directivity and Gain of the BS antennas are the same. It is understood that considering the ohmic losses of the BS antennas requires only to include the efficiency of the antenna in the formulas [15].

As previously indicated, we suppose that the cell has a total number of users equal to P. These users are placed at equi-angular distance $\Delta\theta = 2\alpha/P$. We also suppose that each user covers an angular space equal to $\Delta\theta$. Consequently, P users in the P positions cover the entire $(-\alpha, \alpha)$ range. Finally, we suppose a large number P of users so that the field can be considered approximately constant on $\Delta\theta$. Further notes on P will be given after discussing the model.

We are interested in evaluating the amplitude of the field in one of these positions, let θ_0 be. The user placed in this position will be called the 'reference user' (RU).

The scheduling scheme is the following. The base station firstly serves the RU, and then other $N-1$ users. The time required to complete this process will be defined as 'unit time'. Each of the N receivers is active for a fraction τ of the unit time. Then, the BS serves again the RU, and

then $N-1$ other users different from the users served in the previous unit of time. This process is repeated until all the users are served. In order to serve all the P users the system requires $M = (P-1)/(N-1)$ time units (in the following we will suppose $(P-1)/(N-1)$ integer for sake of simplicity). Consequently, the RU is connected M times in M consecutive unit of times, whereas any other user is connected to the BS only once in M consecutive units of time.

It is understood that the θ_i, $i = 1, .., N$ positions of the active users in the unit time is a subset of the potential positions θ_i, $i = 1, ..., P$ of the total users of the "cell".

The above described model is deterministic. In order to clarify the model, it is useful to make a parallel with statistical models. Basically the scheduling process resembles the 'average' effect of the presence of N active users in the cell, one of them being the RU and the others 'randomly' picked, in case of a very large number of connections. From a statistical point of view, this situation gives an unbalanced number of connections between the RU and the other users. For example, let us suppose that there are P potential users in the cell. If only two users (including the RU) *are connected for each trial*, statistically the number of connections toward RU would be $P/2$, whilst the number of connections with any other user would be $1/(P-1)$. The case $N = P$ (i.e. $M = 1$) models a statistically balanced access to all the users, including RU, in the set of trials. Clearly, the deterministic approach gives a rough model of the communication process in case of small N. For example all the users (including the RU) could be very close to each other during the whole communication process, causing an EMF level on the RU much larger than the one obtained with the deterministic model used in this paper. Statistical models are able to describe these cases. A more detailed analysis of the limitations of the deterministic model will be discussed in the numerical section.

In the following we will call $E(\theta_i, \theta_j)$ the field radiated by the BS antenna in the direction θ_i when the main beam is directed along θ_j. Accordingly the power density is $S(\theta_i, \theta_j) = \frac{|E(\theta_i, \theta_j)|^2}{2\zeta}$ wherein ζ is the free space impedance. Regarding the set of patterns radiated by the BS antenna, we suppose that all the patterns are symmetric with respect to the main lobe and equal apart from an angular rotation, so that $|E(\theta_i, \theta_j)| = |E(\theta_j, \theta_i)| \ \forall \ \theta_i, \theta_j \in (-\alpha, \alpha)$. We will call D the Directivity of the patterns.

The idea at the base of the method proposed in this paper is to compare the power density received in the observation (angular) position θ_0 wherein the RU is placed in two different scenarios.

The first scenario is used as 'reference' and considers an isotropic BS antenna radiating a field amplitude toward the observation point equal to $|E^{iso}|$ wherein iso stands for isotropic case.

The second scenario considers a beam-steering directive antenna, radiating toward the RU (placed in θ_0 direction) the same field amplitude of the isotropic antenna. i.e.:

$$|E(\theta_0, \theta_0)|^2 = |E^{iso}|^2 \tag{1}$$

As discussed above, we are interested in the ratio between the power density in the observation points in the two cases (isotropic and beam steering antennas) in presence of the other users (i.e. $N > 1$). This ratio will be called F_{ant}.

In order to estimate F_{ant} as a first step let us consider an isotropic BS antenna.

During a unit time the BS transmits N uncorrelated signals toward the N active users. Consequently, the average power received per unit time by RU placed in θ_0 in presence of the other $N-1$ receivers is given by N times the power density received in absence of the other receivers:

$$S^{iso} = N \frac{|E^{iso}|^2}{2\zeta} \tau \tag{2}$$

Now, let us suppose that the BS uses a beam steering antenna.

The power density received in the angular direction of the RU, θ_0, is:

$$S_G = \sum_{i=0}^{N-1} \frac{|E(\theta_0, \theta_i)|^2}{2\zeta} \tau \tag{3}$$

wherein the sum ranges from 0 to $N-1$ since it includes both the $N-1$ users at angular positions different from θ_0, and the RU in θ_0.

The ratio between the power received at the RU position and the one received in case of isotropic BS antennas in presence of the other $N-1$ users is approximatively:

$$\frac{\frac{|E(\theta_0,\theta_0)|^2}{2\zeta}\Delta\theta\tau + \sum_{i=1}^{N-1}\frac{|E(\theta_0,\theta_i)|^2}{2\zeta}\Delta\theta\tau}{N\frac{|E^{iso}|^2}{2\zeta}\Delta\theta\tau} =$$
$$\frac{\frac{|E(\theta_0,\theta_0)|^2}{2\zeta}\Delta\theta + \sum_{i=1}^{N-1}\frac{|E(\theta_0,\theta_i)|^2}{2\zeta}\Delta\theta}{N\frac{|E(\theta_0,\theta_0)|^2}{2\zeta}\Delta\theta} \tag{4}$$

In order to cover all the P positions, we need M units of time, obtaining

$$F_{ant} = \frac{M\frac{|E(\theta_0,\theta_0)|^2}{2\zeta}\Delta\theta + \sum_{i=1}^{P-1}\frac{|E(\theta_0,\theta_i)|^2}{2\zeta}\Delta\theta}{NM\frac{|E(\theta_0,\theta_0)|^2}{2\zeta}\Delta\theta} =$$
$$= \frac{(M-1)\frac{|E(\theta_0,\theta_0)|^2}{2\zeta}\Delta\theta}{NM\frac{|E(\theta_0,\theta_0)|^2}{2\zeta}\Delta\theta} + \frac{\sum_{i=0}^{P-1}\frac{|E(\theta_0,\theta_i)|^2}{2\zeta}\Delta\theta}{NM\frac{|E(\theta_0,\theta_0)|^2}{2\zeta}\Delta\theta} =$$
$$= \frac{M-1}{MN} + \frac{\sum_{i=0}^{P-1}\frac{|E(\theta_0,\theta_i)|^2}{2\zeta}\Delta\theta}{N\frac{P-1}{N-1}\frac{|E(\theta_0,\theta_0)|^2}{2\zeta}\Delta\theta} \tag{5}$$

Let us focus our attention on the sum which covers all the $(-\alpha, \alpha)$ interval and let us extend the sum from $(-\alpha, \alpha)$ to $(-\pi, \pi)$.

$$\sum_{i=0}^{P-1}\frac{|E(\theta_0,\theta_i)|^2}{2\zeta} =$$
$$= \sum_{i=0}^{P'-1}\frac{|E(\theta_0,\theta_i)|^2}{2\zeta} - \sum_{i=P}^{P'-1}\frac{|E(\theta_0,\theta_i)|^2}{2\zeta} =$$
$$= \sum_{i=0}^{P'-1}\frac{|E(\theta_0,\theta_i)|^2}{2\zeta} - \Delta_G \tag{6}$$

wherein $P'\Delta\theta = 2\pi$. Note that Δ_G is the power radiated outside the coverage area. Its value depends on the far side-lobes level of the antenna, that for highly directive antennas is quite low.

Substituting Eq. 6 in the second term of Eq. 5 and writing P as $P = \alpha P'/\pi$ we have:

$$\frac{\sum_{i=0}^{P'-1}\frac{|E(\theta_0,\theta_i)|^2}{2\zeta}\Delta\theta}{\frac{N}{N-1}(\frac{\alpha}{\pi}P'-1)\frac{|E(\theta_0,\theta_0)|^2}{2\zeta}\Delta\theta} - \frac{\Delta_G}{\frac{N}{N-1}(\frac{\alpha}{\pi}P'-1)\frac{|E(\theta_0\theta_0)|^2}{2\zeta}\Delta\theta}$$
$$\simeq \frac{\frac{1}{2\pi}\int_{-\pi}^{\pi}\frac{|E(\theta_0,\theta)|^2}{2\zeta}d\theta}{\frac{1}{2\pi}\frac{N}{N-1}(2\alpha-\Delta\theta)\frac{|E(\theta_0,\theta_0)|^2}{2\zeta}} - \Delta'_G \tag{7}$$

wherein we have approximated the sum with the integral.

Now, let us consider the term $E(\theta_0, \theta)$. This is the field observed in θ_0 when the main lobe of the pattern points toward θ. According to the hypothesis on the beams, this is also equal to $E(\theta, \theta_0)$, i.e. the field in θ when the main lobe is toward θ_0. Accordingly,

$$\frac{\frac{|E(\theta_0,\theta_0)|^2}{2\zeta}}{\frac{1}{2\pi}\int_{-\pi}^{\pi}\frac{|E(\theta_0,\theta)|^2}{2\zeta}d\theta} = \frac{\frac{|E(\theta_0,\theta_0)|^2}{2\zeta}}{\frac{1}{2\pi}\int_{-\pi}^{\pi}\frac{|E(\theta,\theta_0)|^2}{2\zeta}d\theta} \tag{8}$$

and Eq. (8) turns out to be the Directivity D of the pattern used to connect the RU [15]. Consequently F_{ant} can be approximated as:

$$F_{ant} \simeq \frac{1}{N}\frac{M-1}{M} + \frac{2\pi(N-1)}{N}\frac{1}{(2\alpha-\Delta\theta)D} =$$
$$\simeq \frac{1}{N}\frac{M-1}{M} + \frac{\pi}{\alpha D} \tag{9}$$

where in the last passage it is assumed that $N \gg 1$ and $2\alpha \gg \Delta\theta$.

The above formula is based on a number of approximations.

The first approximation is that the patterns of the antenna are symmetric with respect to the main lobe and equal under rotation transformation, obtaining

$$|E(\theta_0, \theta)| = |E(\theta, \theta_0)| \tag{10}$$

This symmetry can be obtained in case of circular radiating systems. In case of different antenna geometries, things are more involved, and a shift in the θ domain of the main beam

causes a shift of the pattern not in the angular domain θ, but in a modified domain. In particular in case of a linear phased array the pattern is shifted in the wavenumber domain $\beta d \sin(\theta)$ [15], wherein d is the inter-element distance among the radiating elements and β the free space wavenumber. In this paper we will use Eq. 9 to estimate F_{ant}, approximating $\sin(\theta)$ with θ. The use of not isotropic radiating elements in the BS antenna causes also a variation of the value of $E(\theta,\theta)$ when the main beam ranges in the $(-\alpha, \alpha)$ angular range [15]. The degree of approximation depends on the value of α: the smaller α, the better the approximation.

The second approximation is that the sum can be approximated by the integral in Eq. 7. Note that in the simple model adopted in this paper, the users represent sampling points on the far-field circular observation domain. The problem is consequently the approximation of the Directivity function by a uniform sampling. Using optimal (non uniform) sampling [21] it is possible to reduce the number of samples to slightly more than four times the electrical length of the antenna. However, in our case we have simple uniform sampling and 'rectangular' basis function, so that an oversampling is required in order to have a field approximately constant in $\Delta\theta$. A 'rule of the thumb' is a number of the samples at least 20 times larger than the dimension of the antenna measured in wavelengths. For example, for a linear array having a 8 elements with $0.5\,\lambda$ inter-element distance we need a value of P of the order at least of 100 to have an acceptable approximation of the sum with the integral.

The third approximation supposes that the difference between the integral evaluated in the $(-\pi, \pi)$ and in the $(-\alpha, \alpha)$ is negligible. From a physical point of view, we suppose that the pattern having main beam toward θ_0 radiates negligible fraction of energy outside $(-\alpha, \alpha)$.

Finally, the above results consider a uniform distribution of the users. The analysis of non uniform distributed users is outside the scope of this paper, and is left to future investigation.

Coming back to the Eq. 9, let us consider the case of small N, when the first term of 9 is relevant. As an example, we suppose $N = 2$. Physically, this case models the presence of only 2 users, i.e. the 'RU user' placed in θ_0 and an other user placed in one of the $P - 1$ other possible positions. When we change the position of the latter user, we have $F_{ant} \simeq \frac{M-1}{2M} \simeq \frac{1}{2}$ supposing $P >> N$ (i.e. $M >> 1$) and $\pi/(\alpha D) << 1/2$. In practice, the second term is never completely negligible, and the estimated F_{ant} turns out to be larger than $1/2$. Increasing the number of users per unit time, we have a decrease of the weight of the first term in Eq. 9 compared the second one, and in general a decrease of F_{ant}.

As noted in the Introduction, the most interesting case regards a full loaded cell, i.e. a large number of users. In this case the second term of Eq. 9 is preponderant compared to the first one, obtaining
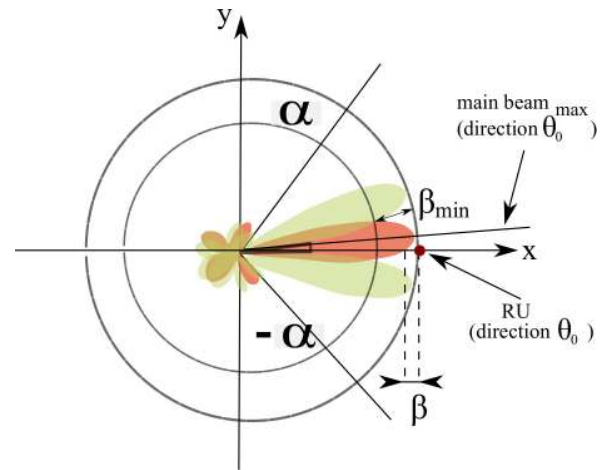
$$F_{ant} \simeq \frac{\pi}{\alpha D} \qquad (11)$$

FIGURE 2. Relevant for the Grid of Beam case; all the beams of the grid are equal apart from an angular rotation; the Reference User (RU) is along $\theta_0 = 0$; the beam having the main lobe closest RU is plotted in red; the direction of this beam is called θ_0^{max}; β is the ratio between the value of the power density of field in the RU direction and along the main lobe in θ_0^{max}; β_{min} is the value of β in the worst case (RU at the intersection direction between two consecutive beams).
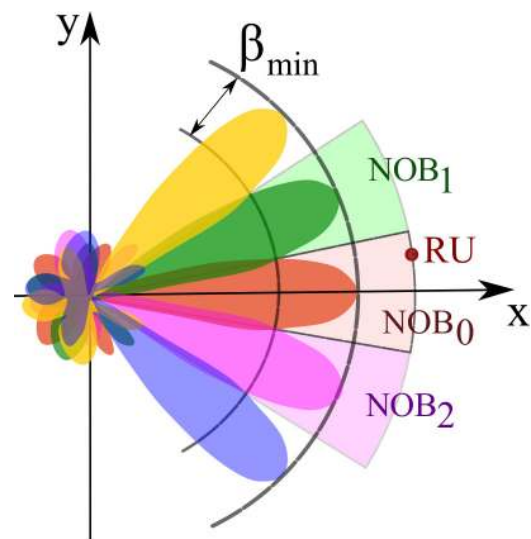

FIGURE 3. The figure shows the NOB (No Overlapping Beam sector) angular range; NOB_i is the NOB relative to the $i - th$ beam; in a grid of beams antenna all the users inside a NOB contribute exactly in the same way to the field impinging on the RU.

and the EMF power reduction turns out to be inversely proportional to the extension of the angular sector served by the BS, and to the Directivity of the antenna.

III. EMF POWER DENSITY REDUCTION USING A GRID OF BEAMS

Antennas radiating a grid of beams are widely used in currently deployed 5G systems. These antennas have a finite set of possible patterns, that partially overlap (see Fig. 2). A user is served by the beam assuring the maximum received power. On the contrary of a beam steering antenna, the maximum of the beam is generally not exactly along the direction of the

RU. Consequently, the power density on the RU is lower than the one along the main lobe by a factor that will be called β. The worst case happens when the user is along the direction of the intersection between two consecutive beams. The value of β in the worst case will be called β_{min} (see Fig. 2) so that β ranges between β_{min} and 1. The angular sector on which the beams do not overlap will be called NOB (No Overlapping Beam sector, Fig.3). The NOB_i is the NOB associated to the $i-th$ beam of the grid of beams. The RU is in the NOB_0.

Paralleling the beam steering case, Eq. 3 is modified as:

$$S_G = \sum_{i=0}^{N-1} \frac{|E(\theta_0, \theta_i^{max})|^2}{2\zeta} \tau \qquad (12)$$

wherein $|E(\theta_0, \theta_i^{max})|$ is the amplitude of the field radiated toward the RU by the pattern whose main beam is closest to the $i - th$ user among all the patterns belonging to the grid of patterns.

Let us consider the following two cases.

In the first case $q - 1$ users are in the NOB_0, wherein also the RU is placed. Independently on the exact position of the users, the RU will received q times the power density compared to the case of presence of only the RU, i.e. $q|E(\theta_0, \theta_0^{max})|^2/(2\zeta)$.

In the second case, the $q - 1$ users are placed in a different NOB, for example the NOB_i $(i \neq 0)$ in which the direction of the main lobe is θ_i^{max}. Again, independently on the exact position of the users in the NOB_i, the RU will receive $q - 1$ times the EM power density $|E(\theta_0, \theta_i^{max})|^2/(2\zeta)$, so that the power density on the RU is $\left((q-1)|E(\theta_0, \theta_i^{max})|^2 + |E(\theta_0, \theta_0^{max})|^2\right)/(2\zeta)$.

In order to have a simple final formula, we approximate $|E(\theta_0, \theta_i^{max})|$ with $|E(\theta_0, \theta_i)|$. As a consequence, in the first case discussed above the power density on the RU caused by the presence of the other users in the NOB_0 is no longer constant, but changes according to the variation of the beam in the NOB. The validity of this approximation depends on the β_{min} value: the closer β_{min} to one, the better the approximation.

Regarding the second case, since the field received in the RU is generally transmitted along the sidelobes of the radiated pattern, we must expect that this approximation could be acceptable. It is understood that the more beams the antenna radiates, the more accurate is this approximation. Numerical simulations reported in Section IV will help to check the approximations above described.

According to these approximations, Eq. (5) changes in:

$$F_{ant} = \frac{\sum_{i=0}^{P-1} \frac{|E(\theta_0, \theta_i)|^2}{2\zeta}}{P \frac{|E(\theta_0, \theta_0^{max})|^2}{2\zeta}} \qquad (13)$$

Extending the sum from $(-\alpha, \alpha)$ to $(-\pi, \pi)$ and supposing that power radiated outside the coverage area is negligible we have:
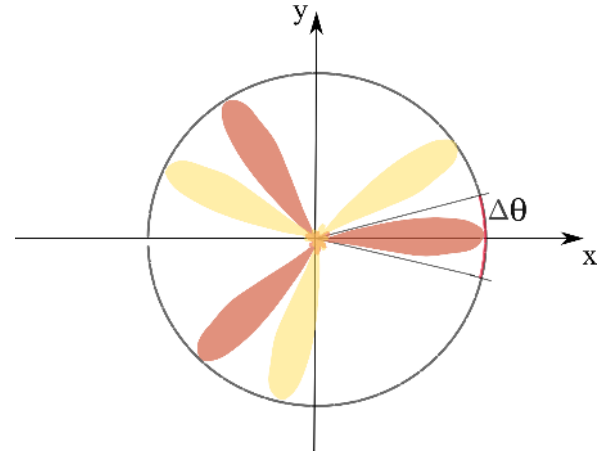

FIGURE 4. An example of MU-MIMO with 3 symmetric main beams $L = 3$ considering two different angular rotations of the MU-MIMO antenna pattern (red pattern and yellow pattern); the MU-pattern must be rotated within a $2\pi/M$ angle to connect all the $N = M L$ users placed on the 2π circumference.

$$\frac{\pi}{\alpha} \frac{\frac{1}{2\pi} \int_{-\pi}^{\pi} \frac{|E(\theta, \theta_0)|^2}{2\zeta} d\theta}{\frac{|E(\theta_0, \theta_0^{max})|^2}{2\zeta}} \qquad (14)$$

wherein $P = \alpha P'/\pi$.

According to the hypothesis on the rotation symmetry of the beams, we have that $|E(\theta, \theta_0)| = |E(\theta, \theta_0^{max})|$, while $|E(\theta_0, \theta_0^{max})| = \beta(\theta_0)|E(\theta_0^{max}, \theta_0^{max})|$. Accordingly:

$$\frac{\frac{|E(\theta_0, \theta_0^{max})|^2}{2\zeta}}{\frac{1}{2\pi} \int_{-\pi}^{\pi} \frac{|E(\theta, \theta_0)|^2}{2\zeta} d\theta} = \frac{\beta \frac{|E(\theta_0^{max}, \theta_0^{max})|^2}{2\zeta}}{\frac{1}{2\pi} \int_{-\pi}^{\pi} \frac{|E(\theta, \theta_0^{max})|^2}{2\zeta} d\theta} \qquad (15)$$

Consequently Eq. 15 turns out to be β times the Directivity D of the pattern used to connect the RU [15], and F_{ant} in case of large number of users can be approximated as:

$$F_{ant} = \frac{\pi}{\alpha D'} \qquad (16)$$

wherein $D'(\theta_0) = \beta(\theta_0)D$. In practice, according to the approximations above discussed, the effect of the use of a grid of beam is equivalent to a reduction of the Directivity in the formula. It is worth noting that D' coincides with the Envelope Radiation Pattern in the direction of the RU [13] .

Finally, recalling that β can range between β_{min} and 1 depending on the direction of θ_0^{max}, a conservative choice for β is $\beta = \beta_{min}$.

IV. EMF POWER DENSITY REDUCTION USING MULTI-USER MASSIVE MIMO ANTENNAS

The MU-mMIMO represents one of the most significant technical advances in 5G. Basically, MU-mMIMO is a Spatial Division Multiplexing Access (SDMA) technique that allows to share the same temporal and frequency resources among many users using antennas having a number of radiating elements much larger that the number of served users.
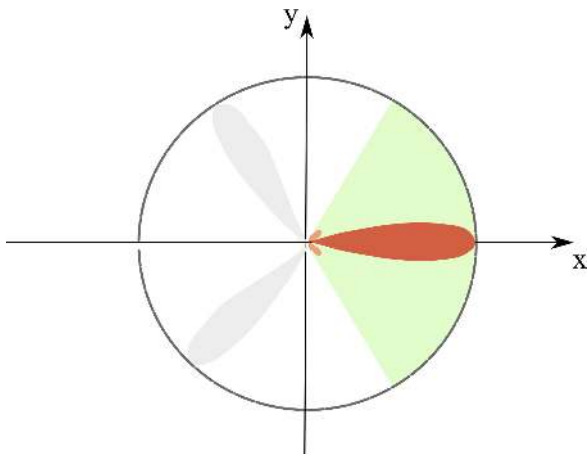
IEEE *Access*

FIGURE 5. The pattern of the MU-mMIMO antenna is the union of the red and the light gray beams plotted in the figure; the pattern of the equivalent antenna used to estimate D' in MU-MIMO is given only by the part of the mu-MIMO pattern inside the green area, having $2\pi/L$ angular extension; consequently the equivalent pattern has a Directivity L times higher than the Directivity of the L-beams MU-mMIMO antenna.

In this paper we will restrict our discussion to MU-mMIMO using one layer for each user. We suppose that the field radiated by the MU-mMIMO is given by the superposition of beam-stearing patterns. Loosely speaking, in free space we can image the far-field configuration of a MU-mMIMO antenna as a multi-main beam pattern, each beam pointing toward a different user [2], [22], [23]. In case of L main-beams, it is possible to connect L users at the same time using L layers, one for each user. We will suppose that the main beams point toward $\theta = 2\pi n/L$ with $n = 0, ..., L-1$ (see Fig. 4).

Even if highly simplified, this model is appropriate for EMF estimation for human exposure assessment in case of non intersecting narrow patterns. This condition is obtained with high probability when the number of users simultaneously served using spatial multiplexing is much less than the number of radiating elements of the antenna, i.e. in case on mMIMO antennas [24].

In order to analyze the MU-mMIMO case let us recall the definition of unit time used in this paper. As defined in the Section 2, a unit time is the time interval between two consecutive connections toward the RU placed in θ_0. In order to avoid to include details that are not fundamental for the discussion, we suppose that the served area α is the entire circumference.

In a L-layer MU-mMIMO system L out of the N users (wherein N is supposed large) are connected with the BS for a fraction τ of the unit time using spatial multiplexing . The scheduling strategy is the following one. Firstly, the RU is served. Thanks to the MU-mMIMO communication characteristics, at the same time other $L-1$ users are also served. Then the pattern is rotated, and other L users are served. We need $H = N/L$ fractions of time τ to connect all the users, after which the RU is served again. Consequently, the unit time is $H\tau$.

In a unit time the ratio between the power received using MU-mMIMO antenna and using an isotropic antenna is:

$$\frac{\frac{|E(\theta_0,\theta_0)|^2}{2\zeta}\Delta\theta\tau}{LH\frac{|E(\theta_0,\theta_0)|^2}{2\zeta}\Delta\theta\tau} + \frac{\sum_{i=1}^{H-1}\frac{|E(\theta_i,\theta_0)|^2}{2\zeta}\Delta\theta\tau}{LH\frac{|E(\theta_0,\theta_0)|^2}{2\zeta}\Delta\theta\tau} \simeq$$

$$\simeq \frac{\frac{1}{2\pi}\int_{-\gamma}^{\gamma}\frac{|E(\theta,\theta_0)|^2}{2\zeta}d\theta}{\frac{|E(\theta_0,\theta_0)|^2}{2\zeta}} \qquad (16)$$

wherein $LH\Delta\theta = 2\pi$ and $\gamma = \pi/L$. The integral is extended only on an angle equal to $2\pi/L$, and includes only one of the L main lobes of the MU-mMIMO antenna.

Due to the symmetry of the MU-mMIMO antenna pattern (see Fig. 4), we have:

$$\frac{\frac{1}{2\pi}\int_{-\gamma}^{\gamma}\frac{|E(\theta,\theta_0)|^2}{2\zeta}d\theta}{\frac{|E(\theta_0,\theta_0)|^2}{2\zeta}} \simeq \frac{1}{L}\frac{\frac{1}{2\pi}\int_{-\pi}^{\pi}\frac{|E(\theta,\theta_0)|^2}{2\zeta}d\theta}{\frac{|E(\theta_0,\theta_0)|^2}{2\zeta}} = \frac{1}{LD} \quad (17)$$

so that

$$F_{ant} \simeq \frac{1}{LD} \qquad (18)$$

Consequently, the reduction factor is the reciprocal of L times the Directivity of the MU-mMIMO.

Let us now suppose that the shape of the main beams of the MU-mMIMO are close to the shape of the main beam of the single-beam configuration, i.e. the total pattern of the MU-mMIMO antenna is the superposition of L single patterns, as shown in in Fig 4. In this case it is advantageous to extend the domain of integration from $(-\gamma, \gamma)$ to $(-\pi, \pi)$ considering an 'equivalent single lobe antenna' whose field is equal to the MU-mMIMO antenna in $(-\gamma, \gamma)$, and negligible outside, as shown in Fig. 5, obtaining:

$$\frac{\frac{1}{2\pi}\int_{-\gamma}^{\gamma}\frac{|E(\theta,\theta_0)|^2}{2\zeta}d\theta}{\frac{|E(\theta_0,\theta_0)|^2}{2\zeta}} \simeq \frac{\frac{1}{2\pi}\int_{-\pi}^{\pi}\frac{|E_{eq}(\theta,\theta_0)|^2}{2\zeta}d\theta}{\frac{|E(\theta_0,\theta_0)|^2}{2\zeta}} = \frac{1}{D_{sb}} \quad (19)$$

wherein D_{sb} is the Directivity of the *single-beam antenna pattern* provided by the vendors (Fig. 5). The value of D_{sb} can be obtained by the plot of the Envelope Radiation Pattern provided by the vendors.

The formulas straightforwardly can be modified to consider a served sector having 2α angular extension, obtaining $F_{ant} \simeq \pi/(\alpha D_{sb})$.

V. EXTENSION OF THE FORMULAS TO THE 3D CASE
The analysis outlined for 2D cases can be easily extended to full 3D geometry.

Let us consider a sphere S surrounding the BS antenna at large distance from the antenna (see Fig. 6). We define a number P of total users on a portion of this sphere having solid angle Ω, and a number N of active receivers in the unit time.
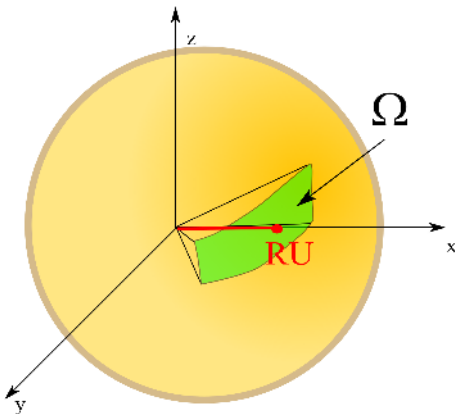
FIGURE 6. 3D model; the users are placed on a section of the spherical surface having solid angular extension Ω; RU is the Reference User, in which position the field reduction is estimated.
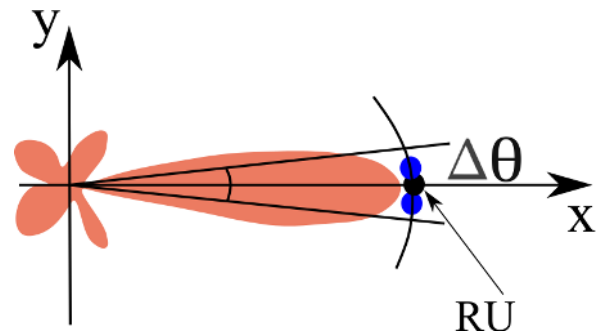

FIGURE 7. A cluster of users is a set of users all placed inside the $\Delta\theta$ interval of the RU; in a statistical distribution model of the users there is a small but not null probability of the presence of clusters of users; the deterministic model considers only one user for each $\Delta\theta$, missing the presence of clusters; the value of the power reduction factor at 95th percentile is quite sensible to the model adopted for the distribution of the users.
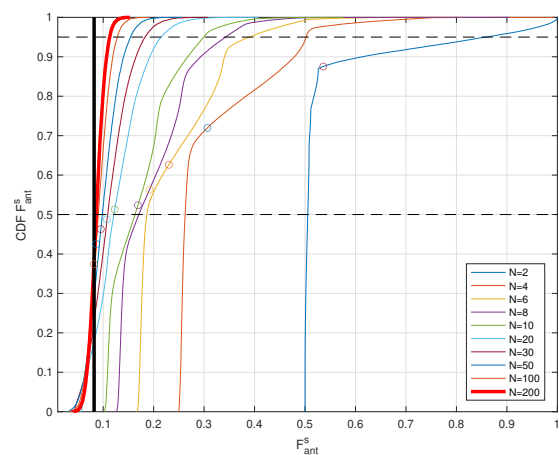
Paralleling the steps followed to estimate F_{ant} in 2D geometry, with trivial modifications it is possible to extend the integral to 3D, obtaining the following approximation in the relevant case of large N we have::

$$F_{ant} \simeq \frac{4\pi}{\Omega}\frac{1}{D_{eq}} \qquad (20)$$

wherein Ω is the solid angle of the domain served by the antenna, and D_{eq} is the Equivalent Directivity, whose value depends on the antenna according to the previous Sections.

This formula can be applied to all the antenna architectures discussed in this paper. It is interesting to note that the value of D_{eq} can be obtained by the Envelope Radiation Pattern [13] . In particular:

- in case of beam steering $D_{eq} = D$, and hence is equal to the Directivity of the beam connecting the user reported in the Envelope Radiation Pattern;
- in case of grid of beam it is approximated as $D_{eq} = \beta_{min}D$, i.e. the minimum Directivity of the Envelope Radiation Pattern;
- in case of MU-mMIMO with single layer per user $D_{eq} = D_{sb}$, i.e. the Directivity of the single-beam antenna pattern as reported in the Envelope Radiation Pattern.

VI. A COMPARISON WITH STATISTICAL APPROACHES

As discussed in the Introduction, the random position of the users makes the estimation of the reduction power factor a stochastic problem. In particular, norms require the estimation of the reduction power factor at 95th percentile. The approach followed in this paper is instead deterministic and is based on a number of approximations and hypothesis. The aim of this Section is to compare the results obtained using the simple deterministic model proposed in this paper with the results of statistical models. Particular attention will be posed to the values at 95th percentile given by statistical approach in case of large number of users.

FIGURE 8. Beam steering case; CDF of the F_{ant}^s in case of 8 elements Uniform Linear Phase Array and $\alpha = \pi/2$; N: number of users that are served in a unit time; the circles are the values obtained using Eq. 9; the value obtained from Eq. 11 (vertical black line) must be compared with the case $N = 200$ (thick red curve).

A. BEAM STEERING ANTENNAS

In order to discuss the numerical results, as a preliminary step let us introduce the concept of a "q users cluster", defined as a cluster of q users (including the RU) all inside the same $\Delta\theta$ of the RU. From a practical point of view, the q users are so close than the RU is almost in the main beam of the other $q-1$ users.

The presence of clusters depends on the statistics adopted to model the user distribution. In general, there is a small but not null probability of having clusters of users. Such a probability determines the value of the power density reduction factor at the highest quantile. For a fixed position of the users, the impact of the presence of clusters to the EMF field receive by the RU depends also on the shape of the beam: the narrower the beam, the smaller the contribution of the other users to the EMF on the RU (see Fig. 7).

In the following the value of F_{ant} obtained using statistical approaches will be called F_{ant}^s, wherein s stands for 'statisti-
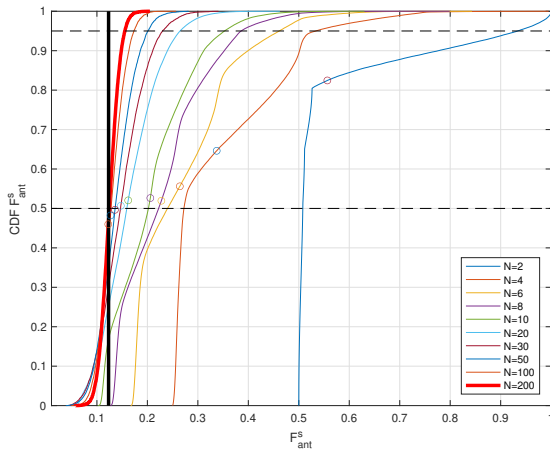
FIGURE 9. Beam steering case; CDF of the F_{ant}^s in case of 8 elements Uniform Linear Phase Array and $\alpha = \pi/3$; N: number of users that are served in a unit time; the circles are the values obtained using Eq. 9; the value obtained from Eq. 11 (vertical black line) must be compared with the case $N = 200$ (thick red curve).

FIGURE 11. Beam steering case; CDF of the F_{ant}^s in case of 16 elements Uniform Linear Phase Array and $\alpha = \pi/3$; $P = 200$; N: number of users that are served in an arbitrary unit time; the circles are the values obained using Eq. 9; the value obtained from Eq. 11 (vertical black line) must be compared with the case $N = 200$ (thick red curve).
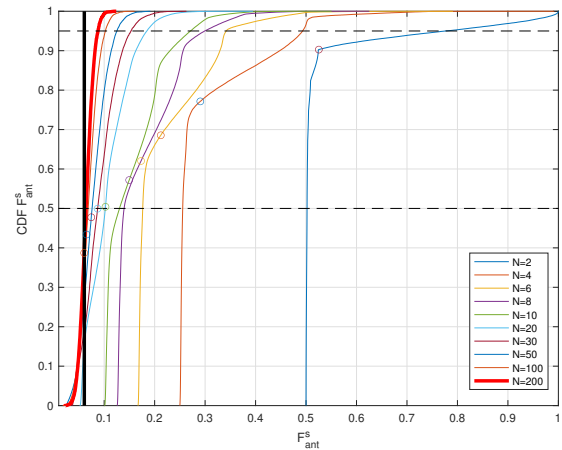

FIGURE 10. Beam steering case; CDF of the F_{ant}^s in case of 16 elements Uniform Linear Phase Array and $\alpha = \pi/2$; $P = 200$; N: number of users that are served in a unit time; the circles are the values obained using Eq. 9; the value obtained from Eq. 11 (vertical black line) must be compared with the case $N = 200$ (thick red curve).
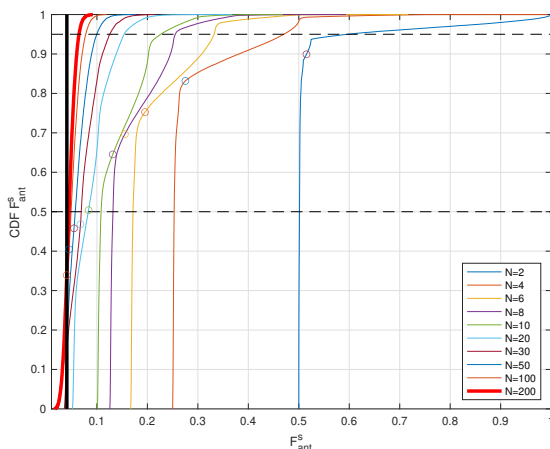
cal'.

The deterministic approach considers only one user for each $\Delta\theta$, and consequently the presence of clusters of users is missed. Accordingly, we must expect a difference between the value obtained by statistical approaches at high quantile and the deterministic approach. This difference depends on the number N of users that are connected in the unit time.

To clarify this point, let us consider the case $N = 2$. The probability that the RU is illuminated by the main beam pointing towards the second user is quite low, giving a reduction factor close to 0.5 in almost all the trails. However, there is a small but not null probability that there are "2 users clusters", i.e. that the two users are so close to be illuminated with almost the same intensity. The closer the users in the

cluster, the greater F_{ant}^s. Consequently, we must expect a transition point at high percentile, before which the reduction power factor is almost 1/2, and after which it has a quite fast increase.

Let us consider now a larger number of users per unit time, for example $N = 4$. With high probability, the RU is not illuminated by the main lobes pointing toward the other three users and $F_{ant}^s \simeq 1/4$. However, there is some probability that there are "2 users clusters", that give a $F_{ant}^s \simeq 1/2$. With lower probability we have also "3 user clusters", that gives an $F_{ant}^s \simeq 3/4$. Finally there is a small but not null probability that there are some "4 users clusters", obtaining a F_{ant}^s value close to the unit. Consequently, the transition between the 'no cluster' condition to 'N cluster' condition, i.e. from $F_{ant}^s = 1/N$ to $F_{ant}^s \simeq 1$, is more gradual than the case $N = 2$.

If N is large, the probability of presence of clusters with a large number of users is quite low, while the effect of clusters having low number of users is moderated by the large value of users served in the unit time. In practice, the value of the power density reduction factor at very high percentile are related to the presence of important clusters. Such clusters depend on the specific model adopted for users distribution [6], [7], and are quite rare in the simulations discussed in this Section, based on an uniform random distribution of the users. Accordingly, in case of large users we must expect that the deterministic model gives a slightly underestimated value of the 95th percentile one. The interested reader can find some examples of the sensitivity of the value of the power density reduction factor for high value of percentile in case of different distributions of users in [6] and [7].

In order to identify the degree of this underestimation, we consider a first group of examples regarding a 2D geometry.

The BS antenna is a Beam Steering Uniform Linear phased Array (ULA) consisting of radiating elements having inter-

element distance equal to 0.5 λ excited considering a uniform amplitude excitation and linear phase, that isotropically radiate in $(-\pi/2, \pi/2)$. A total number of $P = 200$ users are randomly distributed in the $(-\alpha, \alpha)$ angular range. The RU is along $\theta_0 = 0$, i.e. along the broadside direction of the array.

In the first example a beam steering antenna consisting of a ULA having 8 radiating elements with a number of users per unit time ranging from $N = 2$ to $N = 200$ and $\alpha = \pi/2$ is considered. In Fig. 8 the CDF of the F_{ant}^s is plotted for different number of users N served in the unit time. The line of 95th percentile is shown as dotted black line, In the same figures the values obtained using Eq. 9 versus N are plotted as circles. The $\frac{\pi}{\alpha G}$ value is also plotted as solid vertical black line.

The plot confirm the general behavior of F_{and}^s versus N.

In the case of small number of users the statistic of F_{ant}^s is quite far from a Gaussian distribution, with a fast variation of the CDF close to the 95th percentile. As an example, let us consider the case $N = 2$. The CDF is close to 0.5 until the 90th percentile, after which it has a fast increase, reaching 0.85 at the 95th percentile and almost 0.9 at the 97th percentile. The behavior of the curves can be easily explained in terms of presence of clusters of users, as discussed at the beginning of this Section. The position of the transition point is clearly visible.

The plots show an increasing number of 'transition points' when N is increased, moving from a L-like shape curve to a Gaussian CDF like curve in case of large N.

As discussed at the beginning of this Section, the larger the number of users in the unit time, the less probable is the presence of clusters of large number of users. Consequently, when N is large the statistical model tends toward the deterministic model. This behavior is clearly visible in the figure, in which the CDF tends to be highly concentrated on the $\pi/(\alpha D)$ value (vertical solid line in the Figure), making $\pi/(\alpha D)$ a reasonable approximation of the value at 95th percentile for large N.

Now, let us consider the role of the extension of the angular sector that is served by the BS. In the following example, the angular half-sector α is reduced from $\alpha = \pi/2$ to $\alpha = \pi/3$ (Fig. 9, $P = 200$). As first observation, with reference to $N = 2$ we can note that the transition point of the CDF curve is shifted down, from almost 0.9 to about 0.8. This is caused by the smallest served area, that increases the probability of "2 users clusters". This shift in the slope of the curves is also visible in the other curves related to different N values. Considering large N, we can note that the narrower angular sector causes a shift of the CDF curve toward larger F_{ant}^s. This shift is correctly estimated by F_{ant} (vertical black solid line).

In order to analyze the impact of the Directivity, let us consider a larger linear ULA consisting of 16 point-like antenna with $\lambda/2$ inter element distance (Fig. 10). Starting again with the $N = 2$ case, we can note a shift of the transition point toward higher quantile of the CDF curve. This shift is caused
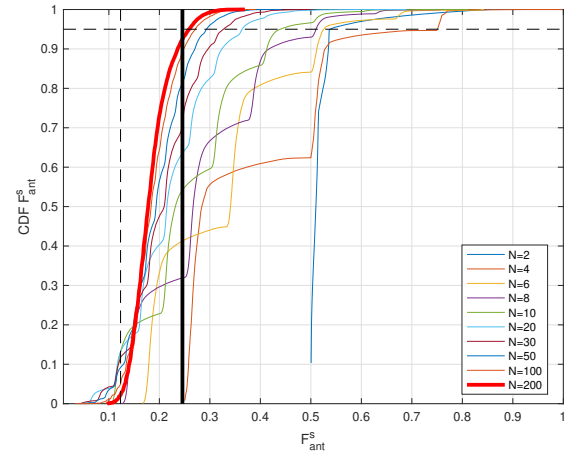

FIGURE 12. CDF of the F_{ant}^s in case of Grid of Beams antenna with beam intersection at 3dB ($\beta = 0.5$), 8 elements Uniform Linear Phase Array, $\alpha = \pi/3$, $P = 200$; N: number of users that are served in a unit time; the value obtained for Eq. 16 (with $D' = \beta_{min} D$) must be compared with the case $N = 200$ (red thick curve); for sake of comparison the value in the case $\beta = 1$ (beam steering antenna) is also drawn (vertical dashed line).

by the reduction of the beamwidth, that reduces the weight of the clusters compared to larger beamwidth antennas. Going to the large N case, narrower beamwidth reduces the fraction of power density radiated toward the RU when the other users are illuminated, with a beneficial effect in terms of EMF power density reduction, as correctly predicted by F_{ant} (vertical black line).

The last example regards the same 16 elements ULA serving a $\alpha = \pi/3$ angular sector (Fig. 11). Again, the results well match with the observation outlined in the above paragraphs. As in the previous examples, Eq. 9 correctly predicts the EMF power density reduction in case of large N.

Generally speaking, the plots show that the proposed formula gives reasonable approximation of the value at 95th quantile in case of large N. In particular, in all the examples reported the relative error is below 10%.

B. GRID OF BEAM ANTENNAS

The above examples regard Beam Steering antennas. Let us now consider the case of Grid of Beams.

As first example we consider an 8 element Uniform Linear Phase Array with $\alpha = \pi/3$, and $P = 200$ using a Grid of Beams consisting of 11 beams with intersection of beams at 3 dB level ($\beta_{min} = 0.5$). Note that the beam serving the RU has the maximum toward $\theta_{max} = 0$ while direction of the RU user θ_0 is randomly placed within the 3 dB beamwidth of the beam with angular uniform distribution. Consequently, in the numerical simulations both the position of the users and the β parameter are random quantities.

The CDF of the F_{ant}^s is plotted in Fig. 12.

Let us analyze the case of small number of user. With reference to the $N = 2$ curve, we can note a sharp transition point, related to the transition between the case in which only
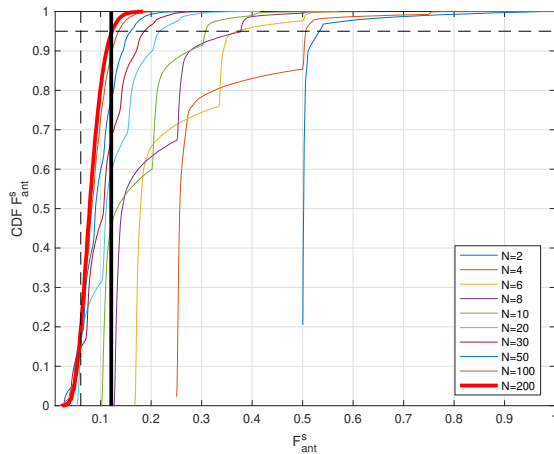
IEEE Access

FIGURE 13. CDF of the F_{ant}^s in case of Grid of Beams antenna with beam intersection at 3dB ($\beta = 0.5$), 16 elements Uniform Linear Phase Array, $\alpha = \pi/3$, $P = 200$; N: number of users that are served in a unit time; the value obtained for Eq. 16 (with $D' = \beta_{min}D$) must be compared with the case $N = 200$ (red thick curve); for sake of comparison the value in the case $\beta = 1$ (beam steering antenna) is also drawn (vertical dashed line).

FIGURE 14. F_{ant} estimated using Eq. 20 versus the D_{eq}; Red line/points: beam-steering antenna, coverage area $30^o \times 120^o$; Green line/points: beam-steering antenna, coverage area $45^o \times 120^o$; Blue line/points: beam-steering antenna, coverage area $60^o \times 120^o$; Solid line: estimated F_{ant}; diamonds: beam-steering antenna, calculated F_{ant} for different coverage area, data from Table 3, Ref [7]; red circles: beam-steering antenna, calculated F_{ant} for different Directivity, data from Table 2, Ref [7]; black points: calculated F_{ant} for MU-MIMO with number of layers ranging from 1 to 8, data from Table 5, Ref [7];

the OE is inside the NOB_0 (obtaining $F_{ant}^s \simeq 1/2$) and the case in both the users are (obtaining $F_{ant}^s = 1$).

In the case $N = 4$ we have 3 transition points. The one at the lowest percentile is associated to transition between the presence of only the OE in the NOB_0 and the presence of two users (including the OE), i.e. from $F_{ant}^s \simeq 1/4$ to $F_{ant}^s \simeq 1/2$. The other points are associated to the transition from two users in the NOD_0 ($F_{ant}^s \simeq 1/2$) to three users ($F_{ant}^s \simeq 3/4$), and from three users in the NOD_0 ($F_{ant}^s \simeq 1/2$) to four users ($F_{ant}^s \simeq 1$). It is understood that the quantile at which we have the transition points depend on the distribution of the users, and distribution different from the uniform one adopted in this paper give different positions of the transition points along the abscissa of the graph.

Now, let us analyze the large N case. The value F_{ant} for large N in case grid of beam case with $\beta = \beta_{min}$ (i.e. $D' = \beta_{min}D = D/2$ in Eq. 16) is plotted as solid black line. For sake of comparison, the value of F_{ant} for large N in case $D' = D$ (beam steering antenna, $\beta = 1$) is plotted in the same figure as a vertical dashed line.

The plot shows that the use of the grid of beam gives a slightly worse EMF power density reduction factor compared to the one using beam sweeping antennas.

The plot shows also that in spite of the rough simplifications at the base of the deterministic model, we have still a reasonable approximation of the EMF power density reduction factor value at higher quantile in case of large N.

As further example, the case of $N = 16$ is shown in Fig. 13. The plot shows a very similar behavior compared to the $N = 8$ case, with a shift of the F_{ant}^s in case of large number of users, fairly well estimated by the analytic approximation formula.
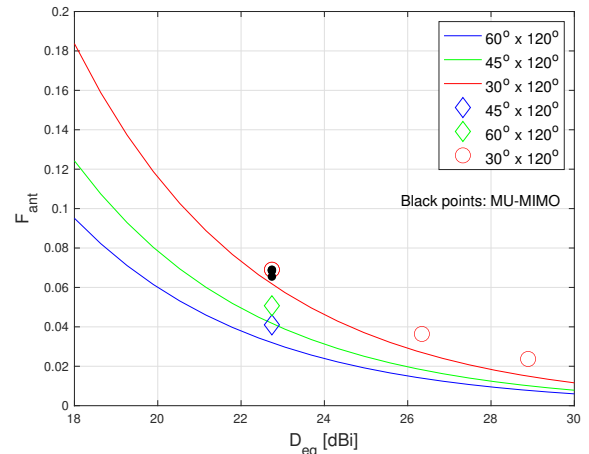
C. MU-MIMO ANTENNA WITH SINGLE LAYER PER USER

Simulations on ULA antennas with 8 and 16 elements with a coverage angle of $2\alpha = 2\pi$ and number of layers equal to $L = 2$ and $L = 3$ have been also carried out using the MU-MIMO model outlined in Section IV.

The plots obtained from the numerical simulations considering users randomly placed on the observation domain are practically identical to the ones shown in Figs. 9 ($L = 2$) and 10 ($L = 3$) and are not reported to save space.

This result well matches with the analysis discussed in Section IV. In fact, according to model adopted for MU-MIMO antenna, a MU-MIMO with single layer per user having $L = 2$ layers and $\alpha = \pi$ (i.e. two beams in the opposite directions) is equivalent to a single-beam array with coverage angle $\alpha = \pi/2$, while a MU-MIMO with single layer per user with $L = 3$ layers and $\alpha = \pi$ (i.e. three beams with maximum along $\theta = 0, 2\pi/3, 4\pi/3$) is equivalent to a single-beam array with coverage angle $\alpha = \pi/3$.

D. COMPARISONS WITH LITERATURE

The above examples regard 2D cases. In the following the results obtained by Eq. 20 are compared with some results reported in the literature using accurate antenna models and Montecarlo analysis in full 3D geometry.

In particular in the following we will check the results given by Eq. 20 with the Q-NAPP at 95th percentile value reported in Ref. [7]. This value coincides with the F_{ant} power reduction factor determined by the antenna pattern [12]. The antenna considered in [7] is a Beam Steering planar phased array with inter-element distance equal to $0.5\,\lambda$. Three different arrays, having 8×8, 12×12 and 16×16 radiating

elements are considered. Regarding the served area, three different cases ($30^o \times 120^o$, $45^o \times 120^o$ and $60^o \times 120^o$) are analyzed.

In order to compare the Q-NAPP value with the simple formula obtained in this paper, as preliminary step in Fig. 14 the value of F_{ant} estimated using Eq. 20 is plotted versus D_{eq} for three different coverage areas: $30^o \times 120^o$ (red solid curve), $45^o \times 120^o$ (greed solid curve) and $60^o \times 120^o$ (blue solid curve). These curves can be applied to different antenna architectures by using the proper value for D_{eq}. In particular, in the following examples, regarding beam steering antennas, D_{eq} is equal to the Directivity of the antenna.

As first comparison, we consider the results in Table 2 of [7], reporting the values of the Q-NAPP (95th percentile, 200 users) in case of the three different antennas and $30^o \times 120^o$ angular sectors. The value of Q-NAPP , plotted as red circle in Fig. 14, must be compared with the red curve estimated using Eq. 20. We can note a good agreement between the analytic curve and the Q-NAPP at 95th percentile obtained by Montecarlo simulations.

As second comparison, we consider the results reported in the first three rows of Table 3, regarding the Q-NAPP (95th percentile, 200 users) in case of an 8×8 array antenna with different covering areas. In particular, the red point in Fig. 14 refers to $30^o \times 120^o$ coverage area, and must be compared with the red curve. The green point in the same figure refers to $45^o \times 120^o$ coverage area, and must be compared with the green curve. Finally, the blue point refers to $60^o \times 120^o$ coverage area, and must be compared with the blue curve. We have again a good agreement between the Q-NAPP and the formula in Eq. 20, confirming that an enlargement of the served angular domain Ω causes a decrease of F_{ant}.

Finally, let us consider the MU-mMIMO case. Ref. [7] analyzes a massive MU-mMIMO antenna with single layer per user consisting of a 8 planar array with $30^o \times 120^o$ coverage area. A number of 200 active user equipment in connected by Spatial Division Multiplexing Access technique with a number of layers varying from 1 (no Spatial Multiplexing) to 8 using an efficient scheduling algorithm [7].

According to the analysis carried out in the previous Section, we can estimate the reduction factor in case of massive MU-MIMO antenna by Eq. 20 considering an equivalent directivity $D_{eq} = D_{sb}$ equal to the directivity of an equivalent single beam antenna, i.e. in the specific case the Directivity of a 8×8 planar array with inter-element equal to 0.5 and uniform excitation, serving the coverage area $30^o \times 120^o$.

The cases of MU-mMIMO using 1, 2, 4 and 8 layers are plotted as black points in Fig. 14 . As discussed above, these values must be compared with the red curve, considering the single-beam case. The plot confirms a good approximation using the formulas obtained by the deterministic model.

Summarizing the results, the maximum relative error in all the cases reported in Fig. 14 using the approximated formula is 37%. This maximum is reached in case of $D = 26$ dBi, for which Q-NAPP is quite low. In terms of maximum absolute error, this turns out to be not larger than 0.01 for all the cases reported in Fig. 14. These values suggest that Eq. 20 could be useful for a fast preliminary evaluation of the power reduction factor.

Of course, the most interesting check of the method proposed in this paper is the comparison with experimental data. At the best knowledge of the authors the only experimental campaign has been described in the interesting paper [8], in which the statistical reduction associated to the antenna is estimated in terms of average of all the Gains of the grid of beams that the antenna can radiate. It is worth noting that, being an experimental procedure, the real patterns of the set of beams of the antenna are considered. Coming back to the numerical results, paper [8] reports a ratio between $\max G_{avr}$ and the peak envelope Gain equal to -8.8 dB (0.13 in natural value). The data have been collected on a commercial 5G network using a 8×8 radiating elements antennas having 0.5λ inter-element distance. The details of the grid of beams of the antennas, including the Directivity, and the angular extension of the coverage area, are not available.

In order to make a comparison, at least at a 'qualitative' level, we can use Eq. 20 supposing a β_{min} between -2 dB and -3 dB and a $30^o \times 120^o$ coverage area. With reference to the red curve in Fig. 14, we must consider the F_{ant} value associated to a Directivity between 2 and 3 dB lower than the one of a 8 planar array, obtaining a value between 0.10 and 0.13, that is compatible with the value reported in [8].

VII. CONCLUSIONS

In the framework of field compliance for human safety the quantity of interest is the power density or the field at the measurement point averaged over a period of time defined by the standards. Starting from the measured data, it is possible to estimate the maximum power using power extrapolation techniques. However, this value is an upperbound, and is not reached in real scenarios. In fact, loosely speaking 5G antennas point the maximum of their lobe toward the user to be served, causing a decrease of the mean value of the power density on the user according to the scheduling strategy adopted by the 5G communication system. Consequently, a further step is required in order to obtain a realistic value of the average power density. This paper is focused on this second step.

Some simple formulas for the estimation of the EMF power density reduction determined by the modern antennas used deployed in 5G communication system are proposed using a simplified deterministic model of a communication system.

In particular it is shown that the power reduction in case of a large number of users can be approximated as $4\pi/(\Omega D_{eq})$ wherein Ω is solid angle of the area served by the antenna, and D_{eq} is an equivalent Directivity depending on the specific antenna system.

The model, developed in details for beam steering and grid of beam antennas, is also extended to analyze the case of MU-MIMO serving L users each with a single layer, showing

that it is possible to use the same approximating formula in which D_{eq} is the Directivity of a single-beam antenna whose main beam has the same shape of the MU-MIMO antenna having L main beams. From a practical point of view, it is possible to apply the reduction parameters to the maximum power value of the EMF field without the explicit knowledge of the number of layers of the MU-MIMO systems. It is also useful to note that the model used for the MU-MIMO antenna supposes that the L beams have all the same shape, and they are positioned at maximum angular distance each to the other. The performance in real systems depends on the details of the beamforming algorithm as well as of the scheduling strategy chosen by the vendor.

The deterministic model adopted in this work was not developed with the aim of replacing the sophisticated statistical models proposed in the literature. As discussed in the paper, the deterministic model is not able to take into account clusters of users, that strictly depends on the specific stochastic model adopted and play an important role in the exact value of the reduction of power density at the highest percentile. However, in spite of the simplicity of the approach, comparison with the results reported in the most recent literature shows that the formulas give a reasonable approximation of the power density in case of large number of users. This behavior, together with the possibility to obtain D_{eq} directly from the plots of the Envelope Radiation Patterns [13], make the formulas proposed in this paper useful for a preliminary fast estimation of the EMF in the 5G cells for human exposure assessment.

REFERENCES

[1] 3GPP, "radio transmission and reception (release 15), 3 gpp technical specification group radio access network; nr, ts 38.104, v15.5.0, may 2019," 2019.
[2] D. Tse and P. Viswanath, *Fundamentals of wireless communication*. Cambridge university press, 2005.
[3] F.-L. Luo and C. J. Zhang, *Signal processing for 5G: algorithms and implementations*. John Wiley & Sons, 2016.
[4] J. Rodriguez, *Fundamentals of 5G mobile networks*. John Wiley & Sons, 2015.
[5] P. Baracca, A. Weber, T. Wild, and C. Grangeat, "A statistical approach for rf exposure compliance boundary assessment in massive mimo systems," in *WSA 2018; 22nd International ITG Workshop on Smart Antennas*. VDE, 2018, pp. 1–6.
[6] B. Thors, A. Furuskär, D. Colombi, and C. Törnevik, "Time-averaged realistic maximum power levels for the assessment of radio frequency exposure for 5g radio base stations using massive mimo," *IEEE Access*, vol. 5, pp. 19 711–19 719, 2017.
[7] D. Pinchera, M. D. Migliore, and F. Schettino, "Compliance boundaries in 5g communication systems: a statistical approach," *EEE Access*, vol. 1, no. 1, pp. 620–628, 2020.
[8] D. Colombi, P. Joshi, B. Xu, F. Ghasemifard, V. Narasaraju, and C. Törnevik, "Analysis of the actual power and emf exposure from base stations in a commercial 5g network," *Applied Sciences*, vol. 10, no. 15, p. 5280, 2020.
[9] S. Persia, C. Carciofi, S. D'Elia, and R. Suman, "Emf evaluations for future networks based on massive mimo," in *2018 IEEE 29th Annual International Symposium on Personal, Indoor and Mobile Radio Communications (PIMRC)*. IEEE, 2018, pp. 1197–1202.
[10] R. Pawlak, P. Krawiec, and J. Żurek, "On measuring electromagnetic fields in 5g technology," *IEEE Access*, vol. 7, pp. 29 826–29 835, 2019.
[11] S. Adda, T. Aureli, S. Coltellacci, S. D'Elia, D. Franci, E. Grillo, N. Pasquino, S. Pavoncello, R. Suman, and M. Vaccarono, "A methodology to characterize power control systems for limiting exposure to electromagnetic fields generated by massive mimo antennas," *IEEE Access*, vol. 8, pp. 171 956–171 967, 2020.
[12] Internation Electromechanical Commission, "Iec 62232:2017, determination of rf field strength, power density and sar in the vicinity of radiocommunication base stations for the purpose of evaluating human exposure." 2017.
[13] N. Alliance, "Recommendation on base station active antenna system standards," 2020.
[14] H. Asplund, D. Astely, P. von Butovitsch, T. Chapman, M. Frenne, F. Ghasemzadeh, M. Hagström, B. Hogan, G. Jöngren, J. Karlsson *et al.*, *Advanced Antenna Systems for 5G Network Deployments: Bridging the Gap Between Theory and Practice*. Academic Press, 2020.
[15] C. A. Balanis, *Antenna theory: analysis and design*. John wiley & sons, 2016.
[16] H. Keller, "On the assessment of human exposure to electromagnetic fields transmitted by 5g nr base stations," *Health physics*, vol. 117, no. 5, pp. 541–545, 2019.
[17] D. Franci, S. Coltellacci, E. Grillo, S. Pavoncello, T. Aureli, R. Cintoli, and M. D. Migliore, "Experimental procedure for fifth generation (5g) electromagnetic field (emf) measurement and maximum power extrapolation for human exposure assessment," *Environments*, vol. 7, no. 3, p. 22, 2020.
[18] ——, "An experimental investigation on the impact of duplexing and beamforming techniques in field measurements of 5g signals," *Electronics*, vol. 9, no. 2, p. 223, 2020.
[19] S. Adda, T. Aureli, S. D'Elia, D. Franci, E. Grillo, M. D. Migliore, S. Pavoncello, F. Schettino, and R. Suman, "A theoretical and experimental investigation on the measurement of the electromagnetic field level radiated by 5g base stations," *IEEE Access*, vol. 8, pp. 101 448–101 463, 2020.
[20] S. Aerts, L. Verloock, M. Van Den Bossche, D. Colombi, L. Martens, C. Törnevik, and W. Joseph, "In-situ measurement methodology for the assessment of 5g nr massive mimo base station exposure at sub-6 ghz frequencies," *IEEE Access*, vol. 7, pp. 184 658–184 667, 2019.
[21] M. D. Migliore, "On the role of the number of degrees of freedom of the field in mimo channels," *IEEE Transactions on Antennas and Propagation*, vol. 54, no. 2, pp. 620–628, 2006.
[22] ——, "On electromagnetics and information theory," *IEEE transactions on antennas and propagation*, vol. 56, no. 10, pp. 3188–3200, 2008.
[23] ——, "An intuitive electromagnetic approach to mimo communication systems [wireless corner]," *IEEE Antennas and Propagation Magazine*, vol. 48, no. 3, pp. 128–137, 2006.
[24] T. L. Marzetta, "Noncooperative cellular wireless with unlimited numbers of base station antennas," *IEEE transactions on wireless communications*, vol. 9, no. 11, pp. 3590–3600, 2010.

• • •